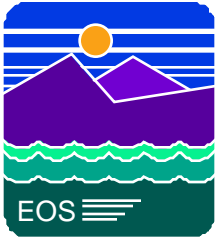




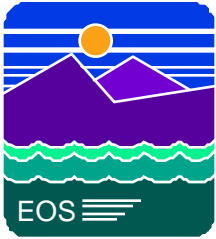
Uncertainties



Uncertainty status and caveats



- Uncertainty model revised
 - improved formalism, designed to focus on “tall poles”
- Uncertainty values not completed
 - numbers here are **very** preliminary
 - input terms based upon data where available; best estimate otherwise
 - subject to significant revision
- Propagation of uncertainties assumes random and normal distributions of errors and no correlations.



Radiance Equation and Uncertainty



$$L_{B,D}(EV) = \frac{DN_{B,D}(EV)}{L_{B,D}(t_{EV})} \quad \frac{L}{L}^2 = \frac{DN^*}{DN^*}^2 + \text{---}^2$$

$L_{EV,B,D}$ Band-averaged spectral radiance from the Earth scene [$W m^{-2} \mu m^{-1} sr^{-1}$]

$DN^*_{EV,B,D}$ Effective count from the detector

$L_{B,D}(t)$ Radiance responsivity from the calibration of MODIS [$counts W^{-1} \mu m sr$]

t Time after the start of on-orbit operations

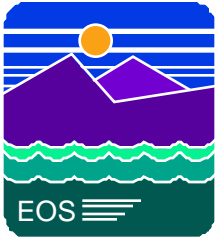
$L_{EV,B,D}$ The band-averaged spectral radiance defined by the equation

$$L_{EV,B,D} = \frac{\int_{\lambda_1}^{\lambda_2} L_{\lambda,EV} R_{\lambda,B,D} d\lambda}{\int_{\lambda_1}^{\lambda_2} R_{\lambda,B,D} d\lambda}$$

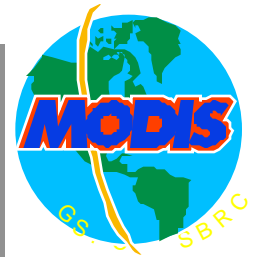
where

$R_{\lambda,B,D}$ Relative spectral response at wavelength

λ_1 and λ_2 Wavelength range over which the detector has a significant quantum efficiency

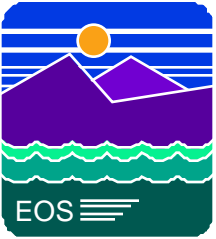


DN* Equation

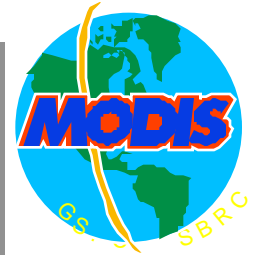


$$DN_{B,D}(EV) = \left[DN'_{B,D}(EV) S_B(MS, F_{AOI=EV}) - \langle DN'_{B,D}(SV) \rangle S_B(MS, F_{AOI=SV}) \right] FF_B(MS, D) \left\{ 1 + K_{B,D} \left[T(FP_B) - T_{CAL}(FP_B) \right] \right\}$$

- DN*** Effective digital counts from the detector after all corrections
- B** MODIS Band
- D** Detector within band B
- DN'** Detector digital counts after correction for Analog to Digital Converter quantization errors.
- EV** Earth View Sector
- SV** Space View Sector
- S** Scan Angle correction for mirror reflectance
- MS** Mirror Side
- F_{AOI}** Frame Angle Of Incidence in the EV or SV sectors
- FF** Flat-Fielding correction to equalize detector response for a given constant scene
- K** Linear correction coefficient for detector response variation with focal plane temperature
- <T(FP_B)>** Average focal plane temperature for a given Band
- T_{CAL}(FP_B)** Reference focal plane temperature for a given focal plane.



DN* Uncertainty



- Assuming uncorrelated error sources that are:
 - random and Normally distributed
 - small enough to require only first order Taylor series expansion about the means

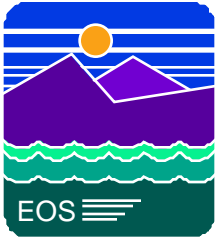
$$\begin{aligned} \frac{DN^*}{DN^*}^2 &= \frac{DN'_{ev}}{dn}^2 S_{ev}^2 + \frac{S_{ev}}{dn}^2 (DN'_{ev})^2 + \frac{DN'_{sv}}{dn}^2 S_{sv}^2 + \frac{S_{sv}}{dn}^2 (DN'_{sv})^2 + \frac{FF}{FF}^2 \\ &+ \frac{K}{\tau}^2 (T - T_{CAL})^2 + \frac{T}{\tau}^2 K^2 + \frac{T_{CAL}}{\tau}^2 K^2 \end{aligned}$$

where we have rewritten the DN* equation for notational simplicity as:

$$DN^*(EV) = [DN'_{ev}S_{ev} - DN'_{sv}S_{sv}] * FF * \{1 + K[T - T_{CAL}]\}$$

and $dn(DN'_{ev}S_{ev}, DN'_{sv}S_{sv}) = DN'_{ev}S_{ev} - DN'_{sv}S_{sv}$

$$\tau(K, T, T_{CAL}) = 1 + K[T - T_{CAL}]$$



Reflectance Equation



$$\rho_{EV,B,D}(t_{EV})\cos(\theta_{EV}) = \frac{\pi L_{B,D}(EV)}{E_{SUN,B,D}}$$

where θ_{EV} is the Earth View Solar zenith angle

$E_{SUN,B,D}$ is the solar irradiance for a given band and detector

A similar expression can be written for the Solar Diffuser (SD) reflectance:

$$\rho_{SD,B,D}(t_{SD})\cos(\theta_{SD}) = \frac{\pi L_{SD,B,D}}{E_{SUN,B,D}}$$

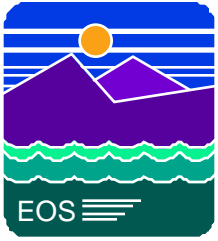
Relating above two equations and accounting for time/Earth-sun distance differences (via t terms) in the reflectance measurements, and introducing an exponential degradation factor for the solar diffuser (with time constant γ):

$$\rho_{EV,B,D}(t_{EV})\cos(\theta_{EV}) = \frac{L_{B,D}(EV)}{L_{B,D}(SD)} \rho_{SD,B,D}(t_{SD})\cos(\theta_{SD}) \frac{(t_{EV})^2}{(t_{SD})^2} e^{-\gamma t_{EV}}$$

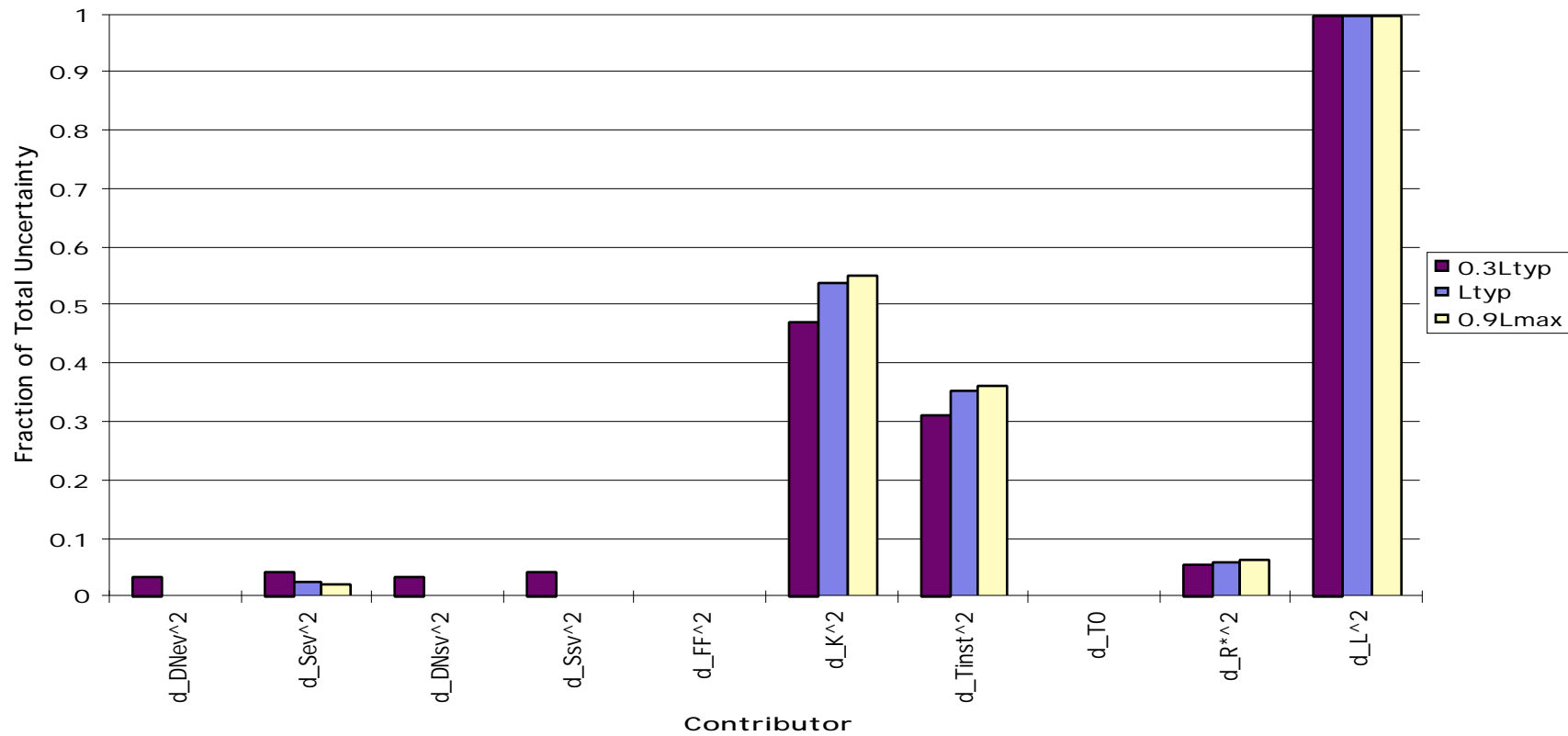
$$\rho_{EV,B,D} \cos(\theta_{EV}) = \frac{DN^*(EV)}{DN^*(SD)} \rho_{SD,B,D} \cos(\theta_{SD}) \frac{(t_{EV})^2}{(t_{SD})^2} e^{-\gamma t_{EV}}$$

Thus the uncertainty in reflectance product becomes:

$$\frac{(\rho_{EV} \cos\theta_{EV})^2}{\rho_{EV} \cos\theta_{EV}} = \frac{DN_{EV}^*{}^2}{DN_{EV}^*} + \frac{DN_{SD}^*{}^2}{DN_{SD}^*} + \frac{(\rho_{SD} \cos\theta_{SD})^2}{\rho_{SD} \cos\theta_{SD}}$$

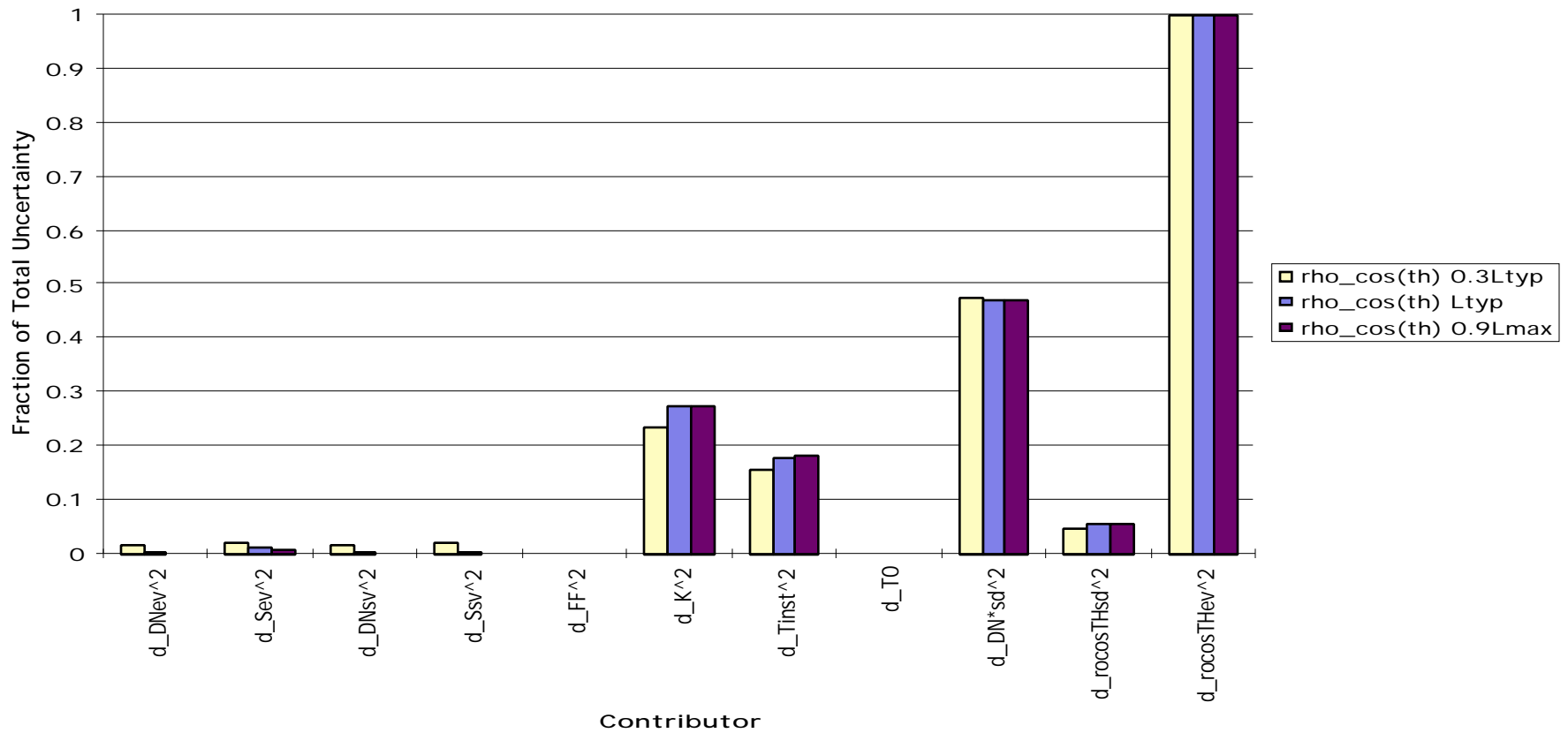


"Tall Pole Analysis" Radiance Product Linear Algorithm Band 10

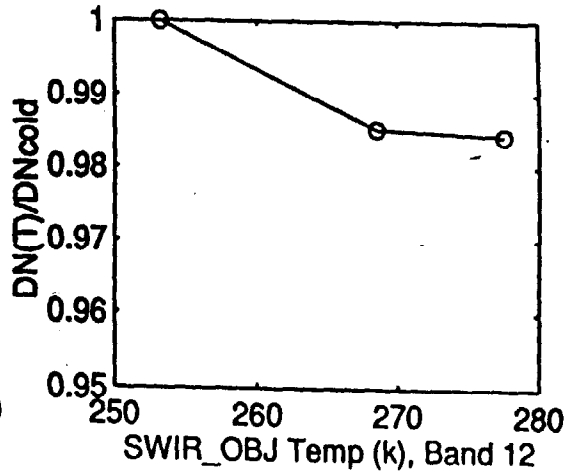
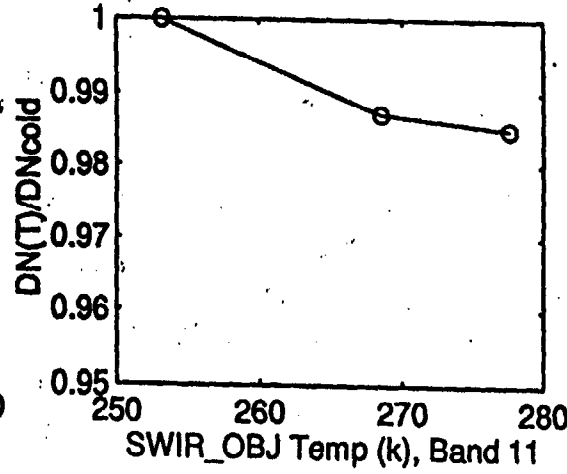
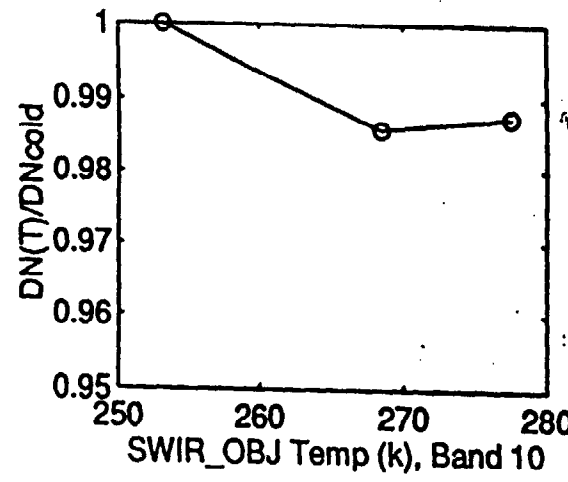
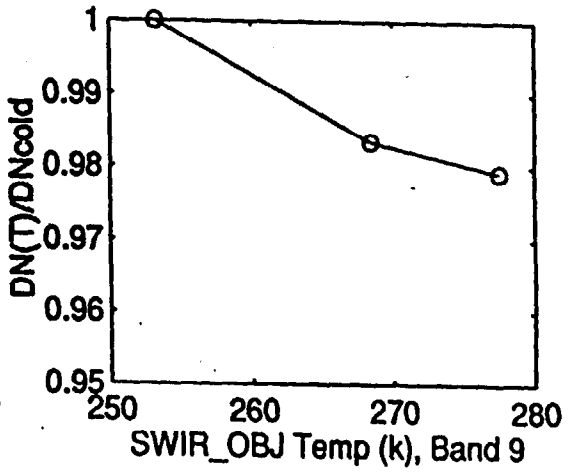
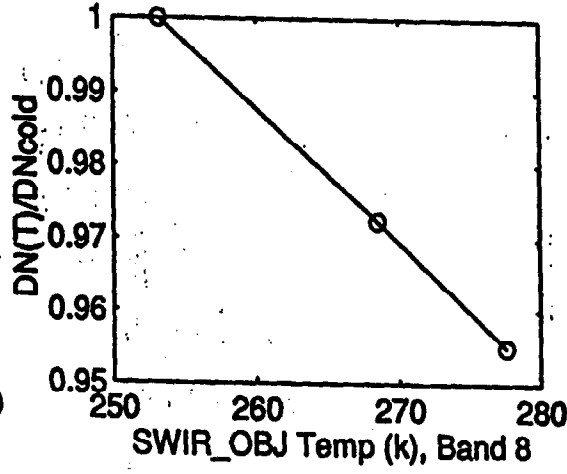
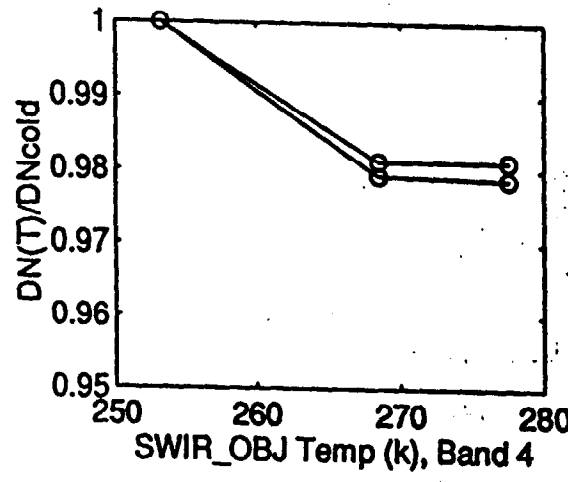
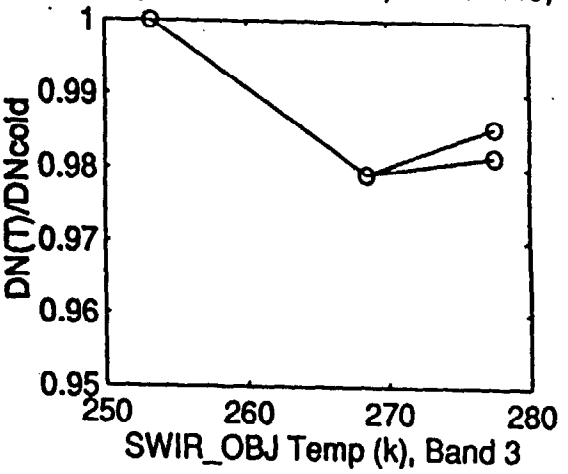
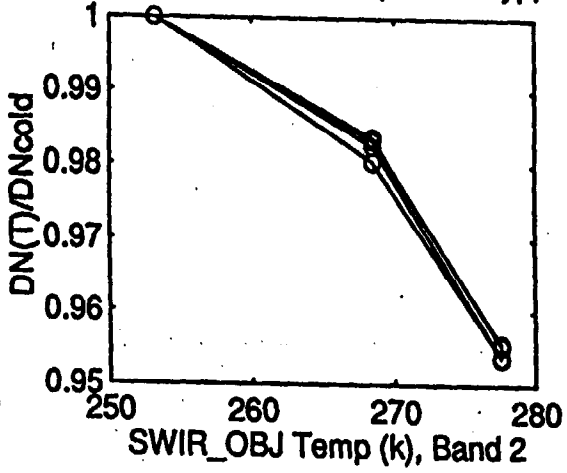
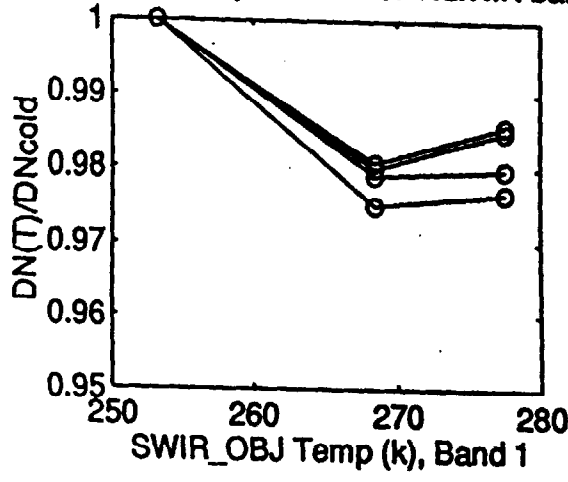




"Tall Pole Analysis" Reflectance Product Linear Algorithm Band 10



Temperature dependence of VIS/NIR bands, middle channel, all samples at L_{typ}, from primary UAID 1338/1339, 1442/1443, 1504



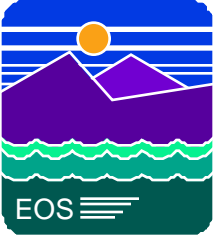


Non-Linear Algorithm and Uncertainties



$$L_{B,D} = a DN_{B,D} + b \left(DN_{B,D} \right)^2$$

$$\frac{L}{L}^2 = \frac{a}{L}^2 \left(DN \right)^2 + \frac{b}{L}^2 \left(DN \right)^4 + \frac{DN}{L}^2 \left(a + 2bDN \right)^2$$



Non-Linear Algorithm and Uncertainties



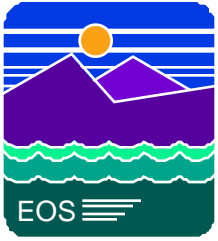
$$\rho_{EV} \cos\theta_{EV} = \frac{aDN_{EV} + b(DN_{EV})^2}{aDN_{SD} + b(DN_{SD})^2} \cos\theta_{SD} \frac{(t_{ev})^2}{(t_{sd})^2} e^{-\tau_{EV}} \rho_{SD}$$

$$\frac{(\rho_{EV} \cos\theta_{EV})^2}{\rho_{EV} \cos\theta_{EV}} = \frac{b^2 (DN_{EV}^*)^2 (DN_{SD}^*)^2 (DN_{SD}^* - DN_{EV}^*)^2}{(aDN_{SD}^* + b(DN_{SD}^*)^2)^2 (aDN_{EV}^* + b(DN_{EV}^*)^2)^2} (a)^2 +$$

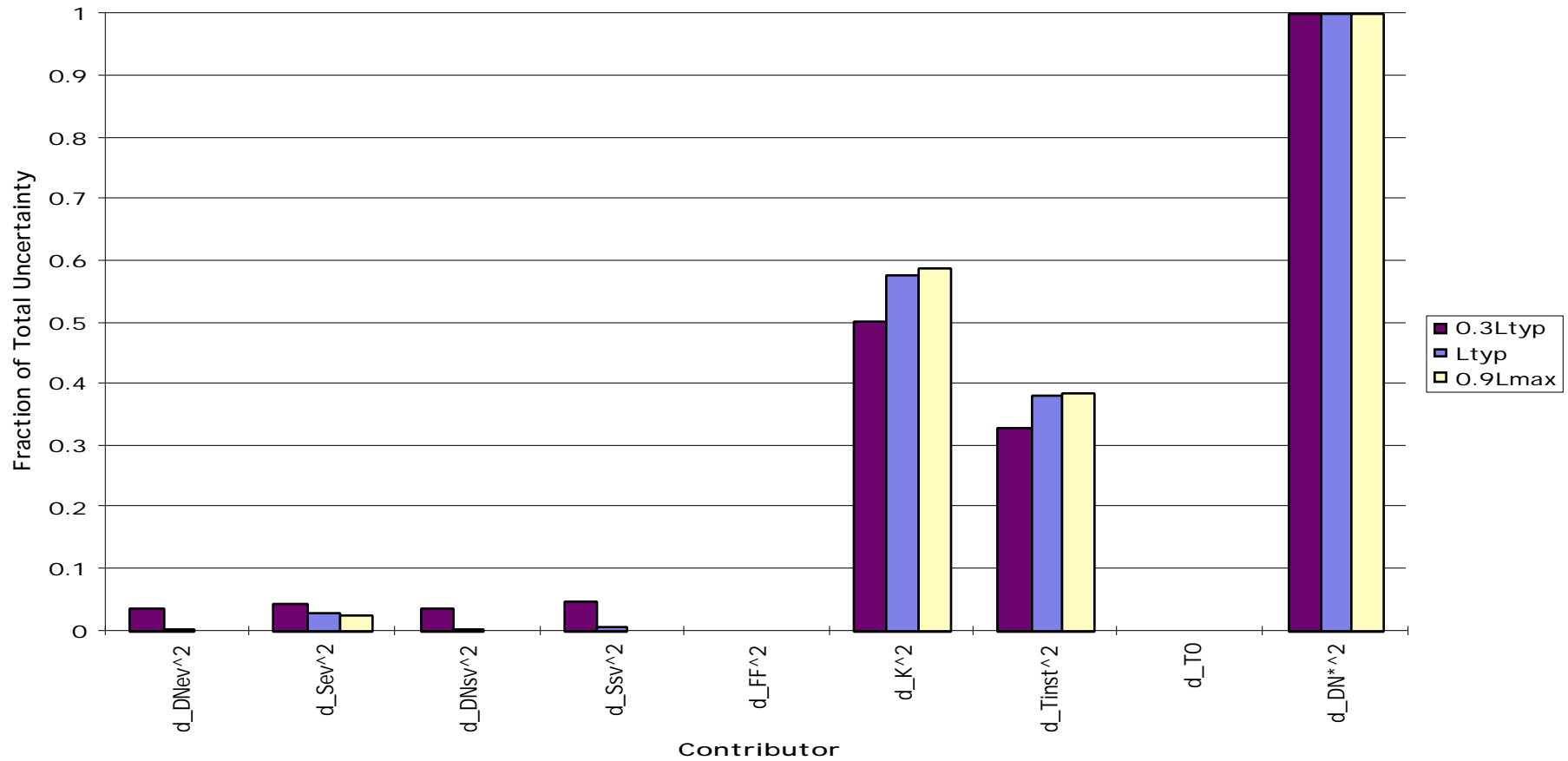
$$\frac{a^2 (DN_{EV}^*)^2 (DN_{SD}^*)^2 (DN_{EV}^* - DN_{SD}^*)^2}{(aDN_{SD}^* + b(DN_{SD}^*)^2)^2 (aDN_{EV}^* + b(DN_{EV}^*)^2)^2} (b)^2 +$$

$$\frac{a + 2bDN_{EV}^*}{aDN_{EV}^* + b(DN_{EV}^*)^2} (DN_{EV}^*)^2 + \frac{a + 2bDN_{SD}^*}{aDN_{SD}^* + b(DN_{SD}^*)^2} (DN_{SD}^*)^2 +$$

$$\frac{(\rho_{SD} \cos\theta_{SD})^2}{\rho_{SD} \cos\theta_{SD}}$$

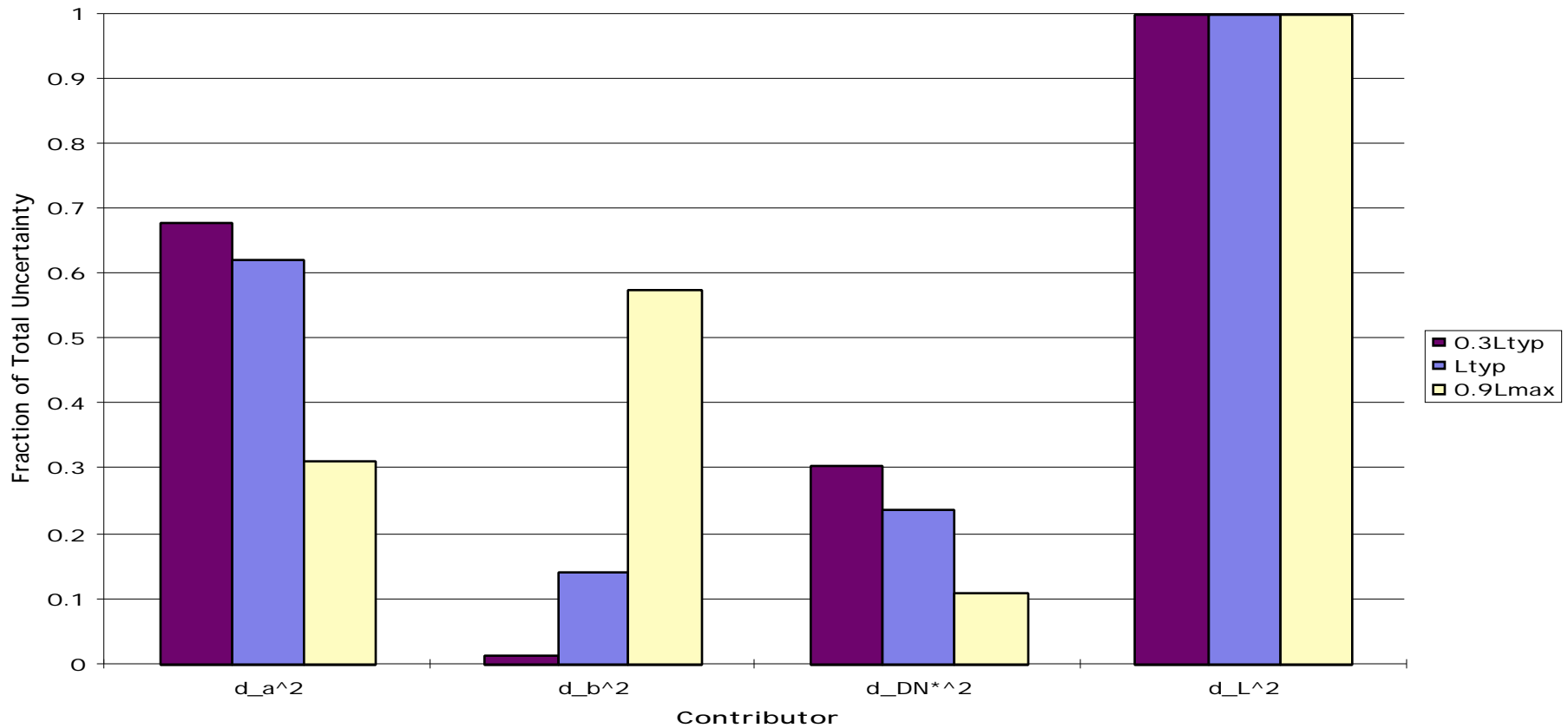


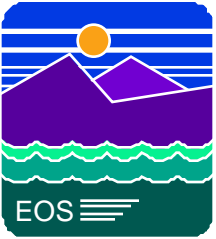
"Tall Poles Analysis" DN* Product Band 10



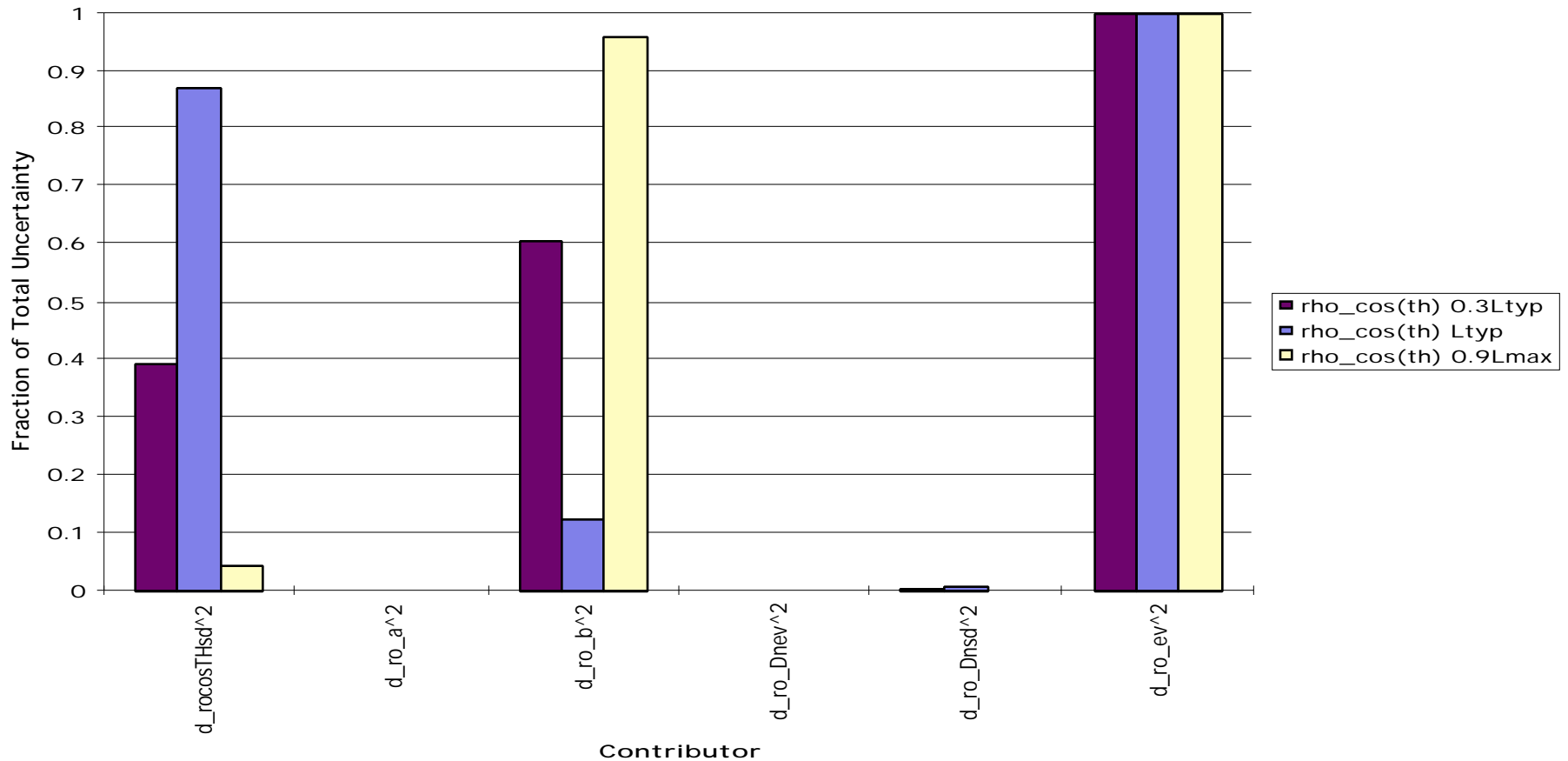


"Tall Poles Analysis" Radiance Product Non-Linear Algorithm Band 10





"Tall Pole Analysis" Reflectance Product Band 10 Non-linear Algorithm



The individual uncertainty elements from Tables II and III were combined (RSS) and the band average are listed in Table IV. Note that three bands, 3, 7, and 26 have significantly lower calibration uncertainty if a third order polynomial is used. These bands and scene levels are encircled.

Table IV. Estimated radiometric calibration uncertainties (total)
for VIS /NIR / SWIR regions

| band | wln (nm) | Total radiometric calib uncertainty | | | | | |
|------|-------------|-------------------------------------|-----------|-------------|-----------|-----------------|-----------|
| | | @ 0.3 L_{typ} | | @ L_{typ} | | @ 0.9 L_{max} | |
| | | 2nd order | 3rd order | 2nd order | 3rd order | 2nd order | 3rd order |
| 1 | 645 | 0.0250 | 0.0231 | 0.0218 | 0.0212 | 0.0206 | 0.0207 |
| 2 | 858 | 0.0210 | 0.0210 | 0.0207 | 0.0206 | 0.0206 | 0.0206 |
| 3 | 469 | 0.0252 | 0.0247 | 0.0238 | 0.0276 | 0.0740 | 0.0384 |
| 4 | 555 | 0.0317 | 0.0306 | 0.0242 | 0.0295 | 0.0239 | 0.0237 |
| 5 | 1240 | 0.0277 | 0.0269 | 0.0252 | 0.0252 | 0.0233 | 0.0233 |
| 6 | 1640 | 0.0243 | 0.0240 | 0.0239 | 0.0240 | 0.0233 | 0.0233 |
| 7 | 2130 | 0.0690 | 0.0582 | 0.0295 | 0.0302 | 0.0235 | 0.0233 |
| 8 | 412 | 0.0263 | 0.0237 | 0.0237 | 0.0244 | 0.0299 | 0.0257 |
| 9 | 443 | 0.0315 | 0.0343 | 0.0247 | 0.0244 | 0.0238 | 0.0238 |
| 10 | 488 | 0.0262 | 0.0238 | 0.0237 | 0.0235 | 0.0235 | 0.0236 |
| 11 | 531 | 0.0238 | 0.0236 | 0.0236 | 0.0236 | 0.0237 | 0.0236 |
| 12 | 551 | 0.0236 | 0.0236 | 0.0236 | 0.0235 | 0.0236 | 0.0236 |
| 13 | 667 | 0.0350 | 0.0285 | 0.0207 | 0.0206 | 0.0206 | 0.0206 |
| 14 | 678 | 0.0381 | 0.0314 | 0.0209 | 0.0206 | 0.0206 | 0.0206 |
| 15 | 748 | 0.0334 | 0.0272 | 0.0206 | 0.0208 | 0.0207 | 0.0221 |
| 16 | 869 | 0.0302 | 0.0287 | 0.0217 | 0.0227 | 0.0206 | 0.0209 |
| 17 | 905 | 0.0235 | 0.0233 | 0.0207 | 0.0207 | 0.0206 | 0.0206 |
| 18 | 936 | 0.0238 | 0.0208 | 0.0298 | 0.0229 | 0.0206 | 0.0206 |
| 19 | 940 | 0.0292 | 0.0243 | 0.0220 | 0.0214 | 0.0206 | 0.0206 |
| 26 | 1375 | 0.0619 | 0.0299 | 0.0301 | 0.0303 | 0.0270 | 0.0271 |